Uniaxial-strain dependence of shear-modulus anomalies in TaS_3

Z. G. Xu and J. W. Brill
Department of Physics and Astronomy, University of Kentucky, Lexington, Kentucky 40506-0055
(Received 18 October 1990)

We have measured the changes in shear modulus and internal friction in TaS_3 when the charge-density wave (CDW) becomes depinned, as a function of uniaxial strain (ϵ), and compared the results with the strain dependence of transport properties. For strains above a critical strain $\epsilon_c \simeq 0.5\%$, where the normal conductivity is a maximum and CDW conductivity a minimum, a second depinning threshold appears, and the elastic anomalies decrease by an order of magnitude. Unlike the case for the conductivity, the low-strain elastic anomalies are not restored by further increases in strain. The results are interpreted in terms of the interaction of a soliton lattice with the CDW.

I. INTRODUCTION

In several materials exhibiting charge-density-wave (CDW) ground states, the CDW can be depinned by application of an electric field greater than a small threshold, E_T. As the CDW becomes depinned, the resistance drops and becomes "noisy"; both broadband ($\sim 1/f$) and narrow-band noise (i.e., voltage oscillations at well-defined frequencies) appear.[1] In most models of the depinned CDW, it is assumed that the extra current is carried by the CDW moving in bulk.[1] Most sliding CDW materials also become elastically "softer" in the depinned state; the dynamic Young's and shear moduli decrease.[2-6] For example, the Young's modulus (Y) (Refs. 2 and 3) of TaS_3 slowly decreases by 2% and its shear modulus (G) (Ref. 4) by 20% as the electric field exceeds E_T. The internal friction associated with both moduli increases rapidly with electric field above E_T, typically reaching maxima of $\sim 0.2\%$ (for Y) (Ref. 2) and 2% (for G) (Ref. 3) at $2E_T$. The Young's modulus anomalies have also been observed to decrease rapidly with increasing (flexural) strain frequency.[7] No model of the elastic properties of the CDW state[8-11] has been successful in explaining the variety of observed effects[5,11] and their surprising frequency dependence.[7]

Equally surprising has been the unusual dependence of the transport properties of TaS_3 on applied uniaxial strain (ϵ). The pinned conductivity (i.e., for $E < E_T$ and due to normal carriers) has a maximum at a sample-dependent strain $\epsilon_c \sim 0.5\%$.[12] At the same strain, E_T changes and the high-field CDW conductivity has a minimum.[13] These results suggested[13] that the non-Ohmic current in TaS_3 is not due to (conventional) bulk motion of the CDW but to motion of an intrinsic array of charged discommensurations, present because the CDW is nearly (fourfold) commensurate,[14] which are also largely responsible for the normal electron scattering. At ϵ_c, it was suggested that the CDW becomes commensurate, increasing the normal electron mobility and reducing the non-Ohmic conductivity.[13] This suggestion was supported by the finding[15] that at ϵ_c the narrow-band noise vanishes, reappearing at larger strain, where the CDW is again incommensurate. An example of this is shown in Fig. 1; for some samples, as shown here, the narrow-band noise spectral features are sharper at large strain than at small.[15,16] It was also observed that near ϵ_c, a second, smaller threshold field appears,[15,16] and it was suggested that the two threshold fields were associated with bulk and discommensuration depinning.[16]

In this paper, we report on measurements of the uniaxial-strain dependence of the shear-modulus anomalies in TaS_3 near 100 K.[17] This work was motivated by the hope that a common investigation of both of these poorly understood phenomena would help clarify them, and the recent report[18] that under small ($\epsilon \sim 0.1\%$) uniaxial strain, the *static* Young's modulus anomaly disappears. We have found that the dynamic ($f \sim 100$ Hz) shear-modulus anomaly varies weakly with strain for $\epsilon < \epsilon_c$; for larger strains, the anomaly decreases by an order of magnitude. Using the elastic rather than the transport anomalies, we were able to trace the evolution of the two threshold electric fields. As for the strain depen-

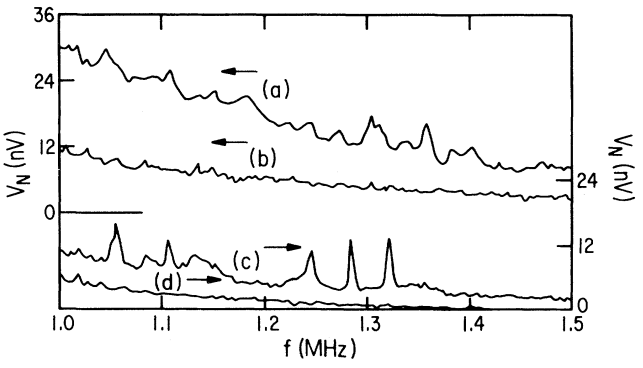

FIG. 1. Noise spectra taken at (a) $\epsilon = 0$, non-Ohmic current $I_{CDW} = 13.1$ μA; (b) $\epsilon = \epsilon_c$, $I_{CDW} = 13.1$ μA; (c) $\epsilon = 5\epsilon_c/3$, $I_{CDW} = 13.1$ μA; (d) $\epsilon = 5\epsilon_c/3$, $I_{CDW} = 0$.

dence of the transport properties, it is difficult to interpret the shear-modulus results in terms of bulk CDW motion alone.

II. EXPERIMENTAL TECHNIQUES

Orthorhombic TaS_3 is a quasi-one-dimensional conductor which undergoes a CDW phase transition into a semiconducting state at 220 K.[1,19] Single crystals, of typical dimensions 10 μm$\times$10 μm$\times$1 cm, were grown by the standard vapor transport technique;[19] the long axis coincides with the high conductivity direction. E_T was typically 0.25 V/cm at 100 K.

Change in the shear modulus was measured by gluing a stiff wire "flag" to the center of a crystal and measuring changes in the resonant frequency f_G (typically 100 Hz) of the resulting "torsional pendulum."[4] One end of the crystal was epoxied to the grounded end of a piezoelectric element and the other end to a sapphire substrate held on a second piezoelectric element. Electrical contact was made to the ends of the sample with silver paint; the contacts were typically separated by 5 mm. For the torsional resonance, $f_G \propto \sqrt{G}$; changes in internal friction are given by changes in the reciprocal quality factor $1/Q$.[4] The resonance was excited by applying voltage to one of the piezoelectric elements, and detected using a helical resonator circuit.[20]

Uniaxial strain was applied with the second piezoelectric element. Because the deflection of the element is a hysteretic function of applied voltage, the latter could not be used to determine the strain. Instead, the frequency of the flexural resonance, f_{FLEX}, excited and detected in the same way as the torsional mode, was used as a relative measure of the strain. For the flexural resonance,[2]

$$f_{\mathrm{flex}} \propto \sqrt{Y[C(a/L)^2+\epsilon]}\ ,$$

where a is the sample thickness, L its length, and C a strain-dependent number of order 1. Hence for $\epsilon \gg (a/L)^2 \sim 10^{-5}$, $\epsilon \propto f^2_{\mathrm{FLEX}}$. This is shown in Fig. 2, for which the piezoelectric voltage is varied monotonically, minimizing hysteresis so $\epsilon \simeq V_{\mathrm{PZ}}$. To establish a relative scale for the strain, the normal low-field resistance R_0 was measured as a function of f_{FLEX}, as shown in Fig. 3. A sharp minimum was observed at a value identified as ϵ_c; although hysteresis was observed in the strain dependent resistance[12,16] (the depth of the minimum usually increased as larger strains were applied), the *location* of the minimum was sufficiently independent of repetition for the critical value of f_{FLEX} to be well defined, e.g., within a few percent. (Creep in the transducer limited the long-term stability of applied strain to $\sim$0.03%.) ϵ_c is apparently sample (and temperature) dependent, varying from 0.4 to 0.7% near 100 K.[12,13,15,16] Strains up to $\sim$1% could be applied without damaging the sample.

After determining the strain scale and approximate values of (strain-dependent) threshold field, the resistance, torsional resonant frequency, and quality factor were simultaneously measured as functions of voltage for several values of strain.[4] The normal (i.e., low-field) tor-

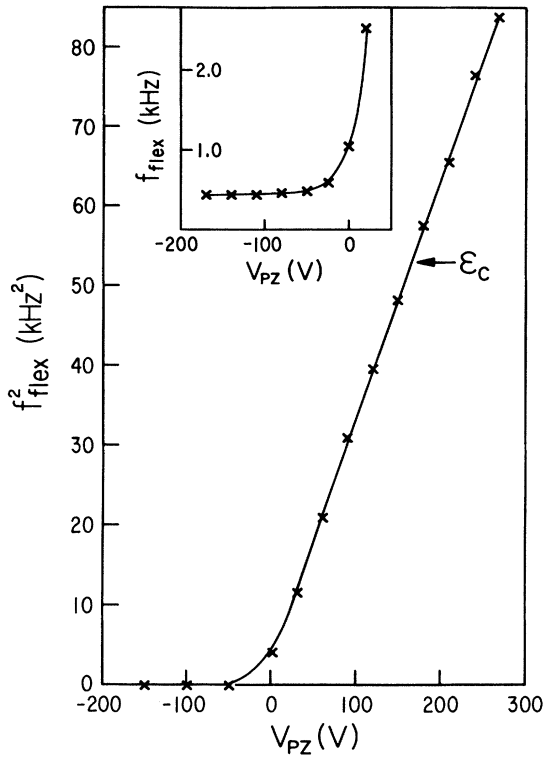

FIG. 2. Flexural resonant frequency vs voltage applied to piezoelectric transducer, taken during a single monotonic sweep to minimize hysteresis in the piezoelectric transducer. The arrow indicates the critical strain (see text). The curve is a guide to the eye. Inset: Enlargement of low-frequency data taken during a separate sweep.

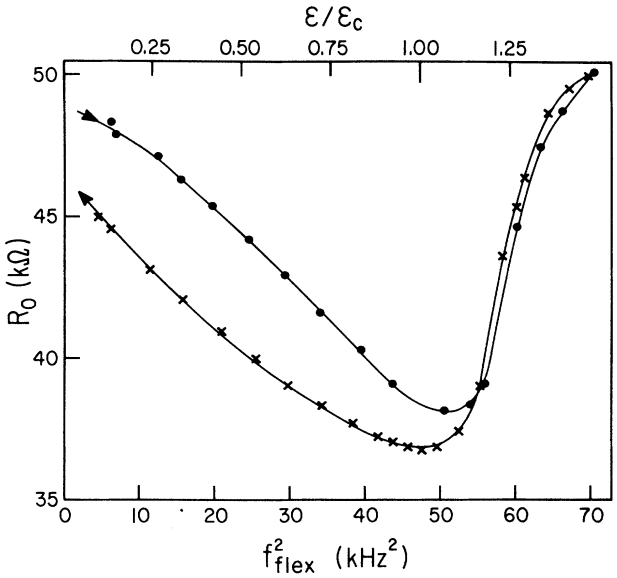

FIG. 3. Normal (low-field) resistance vs flexural resonant frequency; the top scale shows the deduced strains. (Dots: increasing strain; crosses: decreasing strain; curves are guides to eye.)

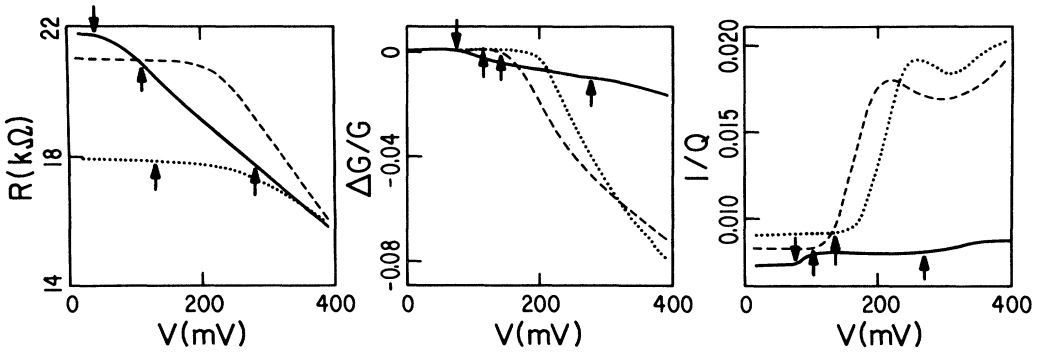

FIG. 4. Resistance, change in shear modulus, and internal friction vs voltage for sample no. 2 at 103 K. (Dashed curves: $\epsilon=\epsilon_c/6$; dotted curves: $\epsilon=5\epsilon_c/6$; solid curves: $\epsilon=4\epsilon_c/3$.) Upward pointing arrows indicate the upper threshold voltages; the second, small threshold at high strain is shown by downward pointing arrows. There are small differences in the threshold voltage observed in different measurements, as described in Ref. 4.

sional resonant frequency was independent ($\pm 2\%$) of strain, and its variation, possibly due to dimensional changes (from Poisson contraction) is ignored below. Most data were taken near 100 K, where E_T^2/R_0, and hence Joule heating, is a minimum. For $E<4E_T$, effects of Joule heating are small and ignored; however, the anomaly in modulus only saturates at $\sim 10E_T$.[4] To find the total modulus anomaly $[G(E\gg E_T)-G(0)]/G(0)$, the frequency shifts were corrected for Joule heating, as described in Refs. 2 and 3.

III. RESULTS

Figures 4 and 5 show the voltage dependence of the resistance, shear modulus, and internal friction at different strains for two samples at 103 K. The arrows indicate the positions of the threshold voltages V_T, where the resistance falls, the modulus decreases, and/or the internal friction increases. The most salient features are (i) the anomalies only vary slowly with strain for $\epsilon<\epsilon_c$, so the absence of a Young's modulus anomaly in Ref. 18 is probably not due to the finite strains ($\sim 0.1\% \sim \epsilon_c/5$) used there, (ii) at high strain, the elastic anomalies are greatly reduced, and (iii) at high strain, two threshold voltages are observed. Similar results were found on all six samples checked.

The total elastic anomalies $[G(0)-G(V\gg V_T)]/G(0)$ and $[1/Q(V\gg V_T)-1/Q(0)]$ at 103 K are shown as functions of strain in Fig. 6. The magnitude of the decreases in elastic anomalies with strain is sample dependent. However, in all cases, the decrease occurs at a strain slightly larger than ϵ_c and the anomalies do not recover for strains up to $1.7\epsilon_c$, the largest applied. In these regards, the elastic anomalies differ from the resistance anomalies, which are (roughly) symmetric about ϵ_c.[12,13,15,16] (The thermoelectric power is also asymmetric about ϵ_c.[16,21])

The presence of two threshold fields slightly above ϵ_c was previously reported,[15,16] but their strain dependence was difficult to determine because both are usually apparent over a limited range in resistance measurements. The two thresholds are more readily observed in the elastic properties, however. The strain dependence of the thresholds at 97 K is shown in Fig. 7. It does not appear as if the lower threshold splits continuously from the

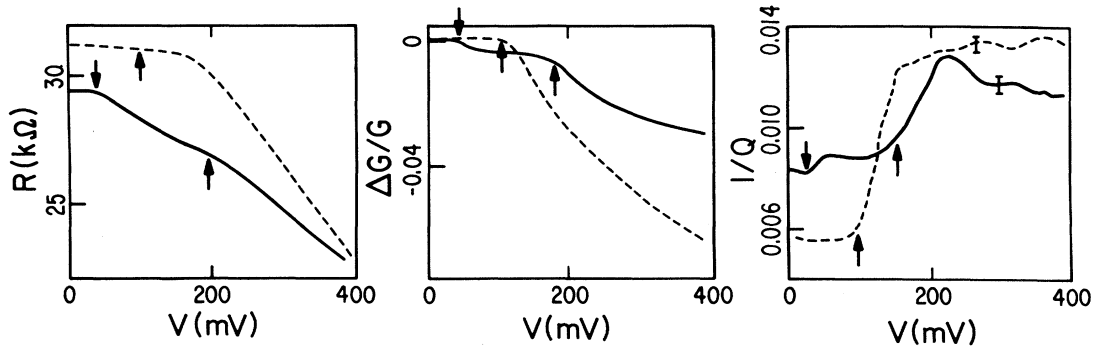

FIG. 5. Resistance, change in shear modulus, and internal friction vs voltage for sample no. 3 at 103 K (Ref. 17). (Dashed curves: $\epsilon=\epsilon_c/3$; solid curves: $\epsilon=3\epsilon_c/2$.) Arrows indicate threshold voltages, as in Fig. 4.

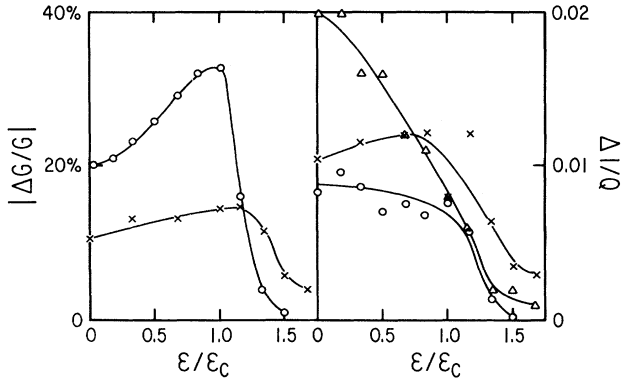

FIG. 6. *Total* shear modulus and internal friction depinning anomalies at 103 K vs strain. (Circles: sample no. 2; crosses: sample no. 3; triangles: sample no. 1; curves are guides to eye only.)

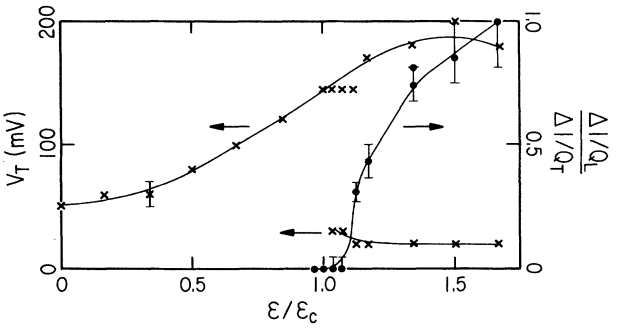

FIG. 7. Strain dependence at 97 K of threshold voltages (crosses) and internal friction anomaly (dots) at lower threshold, normalized to total (see text), for sample no. 4.

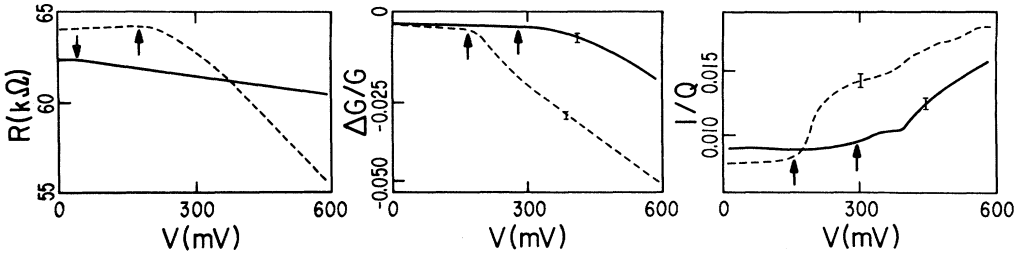

FIG. 8. Resistance, change in shear modulus, and internal friction vs voltage for sample no. 3 at 84 K. (Dashed curves: $\epsilon=0$; solid curves: $\epsilon-3\epsilon_c/2$.) Arrows indicate threshold voltages, as in Fig. 4.

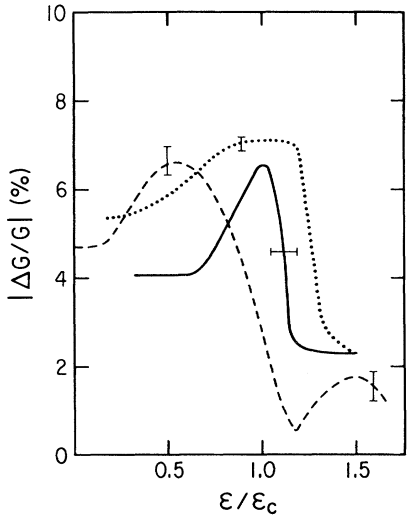

FIG. 9. Strain dependence of shear-modulus anomalies of sample no. 2 at 84 K (dashed curve), 103 K (dotted curve), and 125 K (solid curve). Anomalies are measured at twice the (upper) threshold voltage.

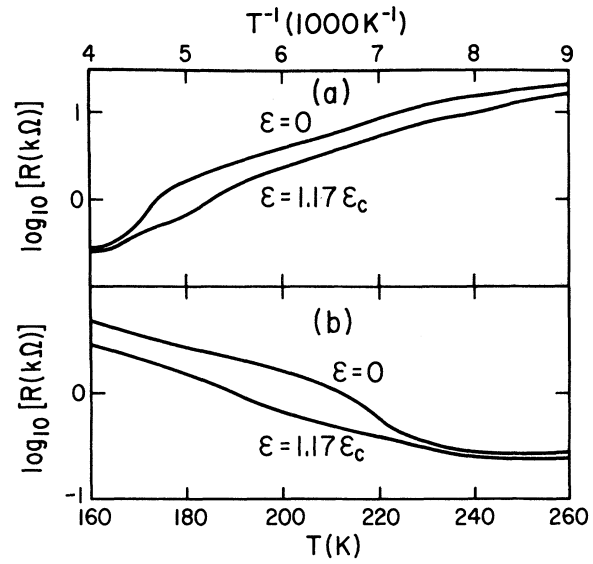

FIG. 10. Temperature dependence of resistance at two strains; ϵ_c is determined at 100 K (Ref. 17).

upper near ϵ_c. Rather, at ϵ_c a small decrease in modulus becomes apparent at the lower threshold. As this anomaly grows, anomalies in internal friction and resistance at the lower threshold become apparent; the resistance anomaly at the upper threshold is already not evident in this sample by $\sim 1.1\epsilon_c$. Because the internal friction anomaly saturates (as a function of voltage) much more rapidly than the modulus anomaly, it is possible to characterize the sizes of the two anomalies in internal friction. This is also shown in Fig. 7, where the magnitude of the lower anomaly, normalized to the total $\{\Delta[1/Q(\text{lower})]+\Delta[1/Q(\text{upper})]\}$ is plotted versus strain. The lower anomalies grow at the expense of the upper with increasing strain for all samples; however, the speed of the growth varies considerably with sample (e.g., compare Fig. 5).

Although most data were taken near 100 K, we also examined the temperature dependence (between 84 and 125 K) of these effects for some samples. No significant change in behavior is observed with increasing temperature. The voltage dependences of the resistance, modulus, and internal friction at two strains at 84 K are shown in Fig. 8. Here, for $\epsilon > \epsilon_c$ the lower threshold is observed only for the resistance; the elastic anomalies at the lower threshold are $<0.1\%$. However, the "total" elastic anomalies continue to vanish with increasing strain, as shown in Figs. 8 and 9. In the latter figure, the strain dependences of the elastic anomalies at 84, 103, and 125 K are compared. (Here, to avoid Joule heating effects, the anomalies are measured at $2V_T$; thus these results are colored by difficulties in identifying the threshold precisely, especially at the lower temperature,[22] and possibly different rates of growth of the anomalies with voltage at different temperatures.)

Finally, we measured the temperature dependence of the (low-field) resistance at constant strain of zero and $1.17\epsilon_c$ (measured at 100 K, where two thresholds were clearly seen), by keeping f_{FLEX} constant as the temperature was varied. The results, shown in Fig. 10, are similar to those of Ref. 12; strain greatly broadens the CDW transition [taken as the maximum[2] in $d\log_{10}(R)/dT$] and slightly increases the activation energy below the transition.

IV. DISCUSSION

Most models of the elastic properties of CDW conductors consider a bulk sliding CDW, and rely on nontrivial changes of the CDW wave vector q with strain, $\Delta q/q \neq -\epsilon$, to account for the depinning anomalies. Such a change in q, in turn, depends on a strain-dependent band structure, e.g., due to strain-dependent interchain coupling, bond hybridization, or charge transfer between inequivalent chains. For example, early models[8] considered decoupling of the effective modulus of the CDW from that of the lattice when the CDW becomes depinned; it was pointed out[4,5] that this can only have effect if q changed nontrivially with strain. Mozurkewich considered relaxational models of the anomalies and pointed out that the most likely possibility was also nontrivial changes in q.[11] In a model proposed by Maki and Virosztek,[9] the elastic anomalies are proportional to the electron-phonon coupling constant, which to be nonzero at the long phonon wavelengths measured also implies a strain-dependent band structure.[5] As mentioned above, none of these models has had complete success in *qualitatively* explaining all effects observed.[5,7,11]

The simplest interpretation of the two threshold fields is that chemically distinct chains become decoupled at ϵ_c, with the lower threshold associated with the smaller shear anomalies (especially at 84 K). A correlation between threshold field and shear-modulus depinning anomaly size was previously observed in $NbSe_3$.[5] Note that although the structure of orthorhombic TaS_3 is not known, inequivalent chains must exist. There are 24 chains per unit cell.[19] If they were chemically equivalent, simple valence considerations indicate that the band would be half (rather than approximately quarter) filled;[23] thus the chains must ge grouped into at least two inequivalent types. The fact that only a single CDW transition is observed (at zero strain) then implies that either only one group of chains is metallic, or that the distortions on different chains are strongly coupled.[1]

Davis *et al.*[16] argued against bulk CDW conduction on different chains giving rise to the two thresholds on the basis of the observation that the ratio of CDW current to narrow-band noise frequency is approximately independent of strain. This ratio is assumed to be proportional to CDW wavelength times condensate density in models of bulk CDW conduction.[1] Their argument is incomplete, however. *Assuming* that the wavelength changes are not large, the ratio should be roughly proportional to the depinned CDW charge moving at a given velocity, which might still be constant, except for the narrow voltage range where two thresholds are observed in the resistance. Here, however, *no* narrow-band noise is observed.

Since Poisson contraction would suggest that chains become more strongly coupled with increasing uniaxial stress, this decoupling must reflect either qualitative changes in pinning potential on different chains or changes in band structure, e.g., charge transfer between chains. The failure to observe a second phase transition in the stressed sample [Fig. 10(b)] argues against these possibilities, although this failure may be due to an increase in ϵ_c near the transition.[16] The weak dependence of activation energy, and presumably CDW gap, on strain [Fig. 10(a)] also argues against significant band-structure changes. Perhaps the strongest argument against a "chain decoupling" model is that, for a bulk CDW, the threshold field is expected to vary inversely with condensate density.[24] Then the finite values for the two thresholds at ϵ_c indicate that the sliding CDW must have a finite amplitude, but the electronic and elastic anomalies vanish.

Thus we are led to the possibility that the lower threshold is not connected to bulk CDW motion. Indeed, the most successful model of the strain dependence of the transport properties of TaS_3 assumes that the non-Ohmic current is carried, at least in part, not by the bulk CDW, but by charged, solitonlike discommensurations,[13–16,23] which vanish at ϵ_c, where the CDW becomes fourfold

commensurate. The two thresholds near ϵ_c may reflect separate depinning of the bulk CDW and the discommensurations, although the lack of symmetry of the (two) thresholds about ϵ_c is baffling.[16] The change in the quality of the narrow-band noise spectrum upon passing through ϵ_c may be due to an interaction between the sliding soliton lattice, which changes sign at ϵ_c, and the sliding bulk CDW.[16] The large change in thermopower at ϵ_c suggests that there is also a strong interaction of the discommensurations and phonons.[16]

There is no model, however, of how a sliding soliton lattice in itself would affect the elastic properties. The presence of large elastic depinning anomalies in $(TaSe_4)_2I$, which is (very) incommensurate, indicates that elastic anomalies can be caused by a sliding bulk CDW, with no discommensurations present, so that the strain-dependent changes may be caused by *changes in the bulk CDW* caused by the solitons. At first sight, the remarkable lack of symmetry about ϵ_c in the elastic anomalies would then seem inconsistent with a lock-in at ϵ_c, with (oppositely charged) discommensurations appearing for both larger and smaller strains. However, a key to eventually reconciling these facts may be the increased coherence of the CDW for $\epsilon > \epsilon_c$, suggested by the sharper narrow-band noise spectrum (Fig. 1).[15,16] While a search for a correlation in CDW coherence and the magnitude of elastic anomalies in *different* samples failed,[5] it was previously found that, within a given sample, the application of a rf signal at the same frequency as the noise, which increases CDW velocity coherence,[1] also decreased the elastic anomalies.[25] Although the mechanism through which interchain CDW phase incoherence can affect the shear modulus (i.e., total interchain coupling) by 20% is far from clear, we assume that such a correlation exists.

We then propose the following scenario. At ϵ_c, the CDW is commensurate, so all the non-Ohmic current and elastic anomalies are associated with the bulk CDW. As discussed above, the growth (from zero) of resistive and elastic anomalies at the lower threshold, which remains finite at ϵ_c, suggests that this is associated with the growth of the soliton lattice as the incommensurability is increased. [Weger and Horowitz[26] suggested that the threshold for the soliton lattice should be smaller (going to zero if no defects are present) than that for the bulk CDW.] The elastic anomalies associated with the motion of the soliton lattice alone are small, vanishingly small at 84 K. The lack of a small threshold for $\epsilon < \epsilon_c$ indicates that solitons of the opposite sign are strongly coupled to the bulk CDW and have the same threshold. This apparent change in soliton interactions with sign may in fact be due to small band structure or pinning potential changes with strain. For the largest strains applied, the solitons sufficiently dominate the transport so that the resistance change due to the comparatively gradual onset of bulk CDW motion at the upper threshold is not apparent; the increased velocity coherence of the CDW also signals the decrease in the elastic anomalies at the upper threshold. Presumably, at even larger strains, when the CDW is sufficiently (probably a few percent[14,23]) incommensurate, the solitons will overlap, and the CDW will become uniformly incommensurate, and a single threshold will be seen.

ACKNOWLEDGMENTS

We appreciate the advice and comments of X.-D. Xiang, G. Mozurkewich, M. J. Skove, E. P. Stillwell, and G. Gruner. This research was supported in part by the National Science Foundation, Grant Nos. DMR-86-15463 and DMR-89-15440.

[1]For reviews, see P. Monceau, *Electronic Properties of Inorganic Quasi-One-Dimensional Compounds,* edited by P. Monceau (Reidel, Dordrecht, 1985), Vol. 2; G. Gruner, Rev. Mod. Phys. **60**, 1129 (1988).

[2]J. W. Brill, W. Roark, and G. Minton, Phys. Rev. B **33**, 6831 (1986).

[3]Ronald L. Jacobsen and George Mozurkewich, Phys. Rev. B **42**, 2778 (1990).

[4]X.-D. Xiang and J. W. Brill, Phys. Rev. B **36**, 2969 (1987).

[5]X.-D. Xiang and J. W. Brill, Phys. Rev. B **39**, 1290 (1989).

[6]G. Mozurkewich, P. M. Chaikin, W. G. Clark, and G. Gruner, Solid State Commun. **56**, 421 (1985); A. Suzuki, H. Mizubayashi, and S. Okuda, J. Phys. Soc. Jpn. **57**, 4322 (1988).

[7]X.-D. Xiang and J. W. Brill, Phys. Rev. Lett. **63**, 1853 (1989).

[8]L. Sneddon, Phys. Rev. Lett. **56**, 1194 (1986); M. S. Sherwin and A. Zettl, Physica D (The Hague) **23**, 62 (1986).

[9]K. Maki and A. Virosztek, Phys. Rev. B **36**, 2910 (1987); A. Virosztek and K. Maki, Phys. Rev. B **41**, 7055 (1990).

[10]R. Zeyher, Phys. Rev. Lett. **61**, 1009 (1988); A. S. Rozhavsky, Yu. S. Kivshar, and A. V. Nedzvetsky, Phys. Rev. B **10**, 4168 (1989).

[11]George Mozurkewich, Phys. Rev. B **42**, 11 183 (1990).

[12]R. S. Lear, M. J. Skove, E. P. Stillwell, and J. W. Brill, Phys. Rev. B **29**, 5656 (1984).

[13]V. B. Preobrazhensky, A. N. Taldenkov, and S. Yu. Shabanov, Solid State Commun. **54**, 399 (1985).

[14]Per Bak, Phys. Rev. Lett. **48**, 692 (1982).

[15]V. B. Preobrazhesnky and A. N. Taldenkov, Synth. Metals **29**, F313 (1989).

[16]T. A. Davis, W. Schaffer, M. J. Skove, and E. P. Stillwell, Phys. Rev. B **39**, 10 094 (1989).

[17]A brief report of these results appears in J. W. Brill and Z. G. Xu, in Proceedings of the International Conference on Science and Technology of Synthetic Metals, ICSM '90 (Tübingen) [Synth. Metals (to be published)].

[18]T. M. Tritt, M. J. Skove, and A. C. Ehrlich, Phys. Rev. B (to be published).

[19]T. Sambongi, K. Tsutsumi, Y. Shiozaki, Y. Yamanoto, K. Yamaya, and Y. Abe, Solid State Commun. **22**, 729 (1977).

[20]X.-D. Xiang, J. W. Brill, and W. L. Fuqua, Rev. Sci. Instrum. **60**, 3035 (1989).

[21]V. B. Preobrazhensky and A. N. Taldenkov, Synth. Metals **29**, F321 (1989).

[22]C. M. Jackson, A. Zettl, G. Gruner, and A. H. Thompson, Solid State Commun. **39**, 531 (1981).

[23]J. A. Wilson, Phys. Rev. B **19**, 6456 (1979).

[24]P. A. Lee and T. M. Rice, Phys. Rev. B **19**, 3970 (1979).

[25]L. C. Bourne and A. Zettle, Phys. Rev. B **36**, 2626 (1987).

[26]M. Weger and B. Horovitz, Solid State Commun. **43**, 583 (1982).